BIOCHEMISTRY
including biophysical chemistry & molecular biology

Article

pubs.acs.org/biochemistry

Site-Selective Monitoring of the Interaction of the SRA Domain of UHRF1 with Target DNA Sequences Labeled with 2-Aminopurine

Vanille J. Greiner,[†] Lesia Kovalenko,[†,‡] Nicolas Humbert,[†] Ludovic Richert,[†] Catherine Birck,[§] Marc Ruff,[§] Olga A. Zaporozhets,[‡] Sirano Dhe-Paganon,[∥] Christian Bronner,[†,§] and Yves Mély*[,†]

[†]Laboratoire de Biophotonique et Pharmacologie, UMR 7213 CNRS, Université de Strasbourg, Faculté de pharmacie, 74 route du Rhin, 67401 Illkirch, France

[‡]Analytical Chemistry Department, Taras Shevchenko National University of Kyiv, 64 Volodymyrska Street, 01033 Kyiv, Ukraine

[§]Institut de Génétique et de Biologie Moléculaire et Cellulaire (IGBMC), INSERM U964 CNRS UMR 7104, Université de Strasbourg, 1 rue Laurent Fries, Illkirch, France

[∥]Department of Cancer Biology, Dana-Farber Cancer Institute, Harvard Medical School, 360 Brookline Avenue, Boston, Massachusetts 02215, United States

S *Supporting Information*

ABSTRACT: UHRF1 plays a central role in the maintenance and transmission of epigenetic modifications by recruiting DNMT1 to hemimethylated CpG sites via its SET and RING-associated (SRA) domain, ensuring error-free duplication of methylation profiles. To characterize SRA-induced changes in the conformation and dynamics of a target 12 bp DNA duplex as a function of the methylation status, we labeled duplexes by the environment-sensitive probe 2-aminopurine (2-Ap) at various positions near or far from the central CpG recognition site containing either a nonmodified cytosine (NM duplex), a methylated cytosine (HM duplex), or methylated cytosines on both strands (BM duplex). Steady-state and time-resolved fluorescence indicated that binding of SRA induced modest conformational and dynamical changes in NM, HM, and BM duplexes, with only slight destabilization of base pairs, restriction of global duplex flexibility, and diminution of local nucleobase mobility. Moreover, significant restriction of the local motion of residues flanking the methylcytosine in the HM duplex suggested that these residues are more rigidly bound to SRA, in line with a slightly higher affinity of the HM duplex as compared to that of the NM or BM duplex. Our results are consistent with a "reader" role, in which the SRA domain scans DNA sequences for hemimethylated CpG sites without perturbation of the structure of contacted nucleotides.

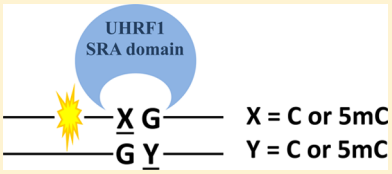

Cell fate is dependent on epigenetic mechanisms that regulate the expression of genes without affecting the DNA sequence. DNA methylation patterns are epigenetic modifications that are set during development and represent "cell memory". One of the first steps of cell division involves recognition of hemimethylated CpG sites generated after DNA replication and duplication by the maintenance DNA methyltransferase DNMT1 of methylation profiles on newly synthesized strands.[1,2] DNA methylation allows regulation of gene expression by inhibiting binding of transcriptional factors to their promoters or inducing recruitment of chromatin remodeling complexes to specific regions of the genome.[3] By being an integral mechanism of differentiation and development, X chromosome inactivation, and genomic imprinting,[4] DNA methylation constitutes a key element in the epigenetic regulation of gene expression.

UHRF1 (ubiquitin-like containing PHD and RING finger 1) is critical in epigenetic code transmission because it mediates modifications of DNA and histones. UHRF1 possesses a SET and RING-associated (SRA) domain that recognizes hemimethylated DNA,[5−13] and a tandem Tudor domain (TTD) and a plant homeo domain (PHD), which can read histone modifications.[14−17] By recruiting various epigenetic regulators to specific chromatin regions, UHRF1 maintains and transmits epigenetic information.[18−20] During replication, UHRF1 contributes to the duplication of DNA methylation profiles by loading DNMT1 to hemimethylated CpG sites, allowing proper methylation of target cytosines on complementary DNA strands.[7,12,21−24] In line with the function of UHRF1, the SRA domain was shown to preferentially bind hemimethylated DNA over nonmethylated and fully methylated DNA.[5−11] The crystallographic structure of the SRA domain in complex with hemimethylated DNA revealed a handlike mechanism that grabs duplex DNA, nestling the flipped-out methylcytosine within its palm.[5,6,9] A short protein loop, termed the thumb, was found inserted into the minor groove and likely promotes methylcytosine base flipping. Opposite to the thumb, a long loop, topped by residues Asn-Lys-Arg, termed the NKR finger, was inserted into the major groove loop, stabilizing the other three bases of the CpG duplex, and filling the hole created by

Received: April 18, 2015
Revised: September 10, 2015
Published: September 14, 2015

DOI: 10.1021/acs.biochem.5b00419
Biochemistry 2015, 54, 6012−6020

the flipped base. This base flipping mechanism is nonenzymatic and confers to UHRF1 the ability to anchor DNA at strategic positions facilitating the recruitment of DNMT1 to hemimethylated CpG sites.[25]

Poorly understood though are the dynamics of the nucleobases in contact with the SRA domain and SRA-induced conformational changes in hemimethylated DNA sequences with those in their nonmethylated or fully methylated counterparts. These dynamical properties of interaction could provide insights into the efficiency and processivity of epigenetic replication by this protein. To address these questions, we investigated the interaction of the UHRF1 SRA domain with 12 bp duplexes substituted at various positions with 2-aminopurine (2-Ap). The 2-Ap is a fluorescent analogue of adenine that can be incorporated within DNA to substitute a natural base, playing the role of a fluorescent reporter that does not significantly disturb the DNA structure or the interactions of DNA with proteins.[26−38] This probe is highly sensitive to its microenvironment, especially to stacking interactions, providing information about its local environment.[39−44] In our study, the introduction of 2-Ap at various positions allowed us to site-specifically investigate the changes in dynamics and conformational changes accompanying SRA binding and to correlate these changes with the known three-dimensional structure of the SRA/DNA complex.[5,6,9] Our findings suggest that SRA domain binding preserves global duplex conformations, inducing similar albeit minor conformational and dynamical changes in nonmethylated, hemimethylated, and fully methylated DNA.

MATERIALS AND METHODS

Materials. The SRA domain of hUHRF1 (SRA, residues 408−643) was expressed in *Escherichia coli* BL21-pLysS(DE3) and purified as described previously.[45] Unmodified or labeled oligonucleotides (ODNs) were synthesized and purified via high-performance liquid chromatography by IBA Gmbh Nucleic Acids Product Supply. The sequence of the used 12 bp duplex ODN was 5′-GGGCCXGCAGGG-3′/5′-CCCTG-YGGGCCC-3′. This sequence was either unmethylated (X = Y = C), hemimethylated (X = 5mC, and Y = C), or fully methylated (X = Y = 5mC). This sequence found in the *RB1* gene promoter is identical to that used by Avvakumov et al.[6] for the structure determination of the SRA/DNA complex. A 2′-deoxyribosyl-2-aminopurine (2-Ap) was selectively introduced at different positions (3, 5, 6, 7, 8, 9, 8′, 7′, 6′, or 5′) to substitute the corresponding natural base within the sequence. Complementary strands were mixed in equal molar amounts in 25 mM Tris-HCl (pH 7.5), 150 mM NaCl buffer and annealed by being heated at 90 °C and then cooled at room temperature. Absorption spectra were recorded on a Cary 400 spectrophotometer. Extinction coefficients between 86500 and 135020 M^{-1} cm^{-1} were used to determine the concentrations of duplex ODNs at 260 nm. The spectra were corrected for diffusion and buffer absorption. All experiments were performed at 20 °C in 25 mM Tris-HCl (pH 7.5), 50 mM NaCl, 0.5 mM PMSF, and 2 mM TCEP, in the presence of 0.04% PEG 20000 to prevent protein adsorption on the cuvette walls.[46]

Steady-State Fluorescence Spectroscopy. Fluorescence emission spectra were recorded at 20 °C on a FluoroMax-3 or FluoroLog spectrofluorimeter (Jobin Yvon) equipped with a thermostated cell compartment. The excitation wavelength was 315 nm to excite selectively the 2-Ap. Spectra were corrected for screening effects, buffer fluorescence, lamp fluctuations, and the wavelength dependence of the optical elements in the emission pathway. Quantum yields of the labeled duplexes in the absence or presence of the SRA protein were determined by taking free 2-Ap riboside as a reference (quantum yield of 0.68[38]). Measurements were performed on 3 μM ODN duplexes in the absence or presence of 4 μM SRA protein.

Time-Resolved Fluorescence Spectroscopy. Time-resolved fluorescence measurements were performed with the time-correlated, single-photon counting technique, as previously described.[26,47,48] Excitation pulses were generated by a pulse-picked frequency-tripled Ti-sapphire laser (Tsunami, Spectra Physics) pumped by a Millenia X laser (Spectra Physics). The excitation wavelength was set at 315 nm, with a repetition rate of 4 MHz. The fluorescence emission was collected through a polarizer set at the magic angle and a 16 mm band-pass monochromator (Jobin Yvon) at 370 nm. The single-photon events were detected with a microchannel plate photomultiplier (Hamamatsu) coupled to a pulse preamplifier HFAC (Becker-Hickl) and recorded on a SPC-130 board (Becker-Hickl). To confidently recover the fluorescence lifetimes from the intensity decays,[49] a minimum of 10^6 photons were collected. The instrumental response function (IRF) was recorded using a polished aluminum reflector, and its full width at half-maximum was ∼50 ps.

The mean lifetime, $\langle\tau\rangle$, was calculated from the individual fluorescence lifetimes (τ_i) and their relative amplitudes (α_i) according to the equation $\langle\tau\rangle = \sum\alpha_i\tau_i$. The population, α_0, of dark species of 2-Ap in the labeled duplexes was calculated with the equation $\alpha_0 = 1 - \tau_{free}/(\tau_{ODN}R_m)$, where τ_{free} is the lifetime of the free 2-Ap, τ_{ODN} is the measured mean lifetime of 2-Ap within the ODN duplex, and R_m is the ratio of their corresponding steady-state fluorescence intensities ($R_m = I_{free2Ap}/I_{ODN}$). The remaining amplitudes, α_{ic}, were recalculated from the measured amplitudes according to the equation $\alpha_{ic} = \alpha_i(1 - \alpha_0)$.

Fluorescence anisotropy decay curves were recorded by cycles of 60 s, alternatively in vertical and horizontal positions of the polarizer, until 1.5×10^6 photons were collected on the $I_{\parallel}(t)$ channel. The signals of both channels were then analyzed by the following equations:

$$I_{\parallel}(t) = I(t)\frac{1 + 2r(t)}{3}$$

$$I_{\perp}(t) = I(t)\frac{1 - r(t)}{3}$$

$$r(t) = \frac{I_{\parallel}(t) - G \times I_{\perp}(t)}{I_{\parallel}(t) + 2G \times I_{\perp}(t)} = r_0 \sum_i \beta_i e^{-t/\varphi_i} \quad (1)$$

where β_i terms are the amplitudes of rotational correlation times φ_i, $I_{\parallel}(t)$ and $I_{\perp}(t)$ are the intensities collected at emission polarization parallel and perpendicular, respectively, to the polarization of the excitation beam, r_0 is the initial anisotropy value, and G is the geometry factor at the emission wavelength, determined in independent experiments. Assuming a rodlike shape for the duplexes, we could calculate the theoretical rotational correlation by

$$\varphi = \frac{\pi L^3 \eta}{4p^2 kT} \quad (2)$$

DOI: 10.1021/acs.biochem.5b00419
Biochemistry 2015, 54, 6012−6020

where L is the rod length, p is the length to diameter ratio, η is the viscosity, k is the Boltzmann constant, and T is the temperature.[50]

Time-resolved intensity and anisotropy data were analyzed by using both the maximum entropy method (MEM)[51] and a nonlinear least-squares analysis using a Levenberg−Marquardt algorithm[52] (kindly provided by G. Krishnamoorthy). The values obtained by both methods were highly consistent. In all cases, the χ^2 values were close to 1, and the weighted residuals as well as the autocorrelation of the residuals were distributed randomly around zero, indicating an optimal fit.

Fluorescence Resonance Energy Transfer (FRET). The SRA (408−643) domain was labeled with Cy3 (Amersham Cy3Maleimide Monoreactive dye 5-pack) on Cys 497 and purified by gel filtration (Superdex 200). ODNs were labeled with Cy5 at the 5′ end (IBA Gmbh Nucleic Acids Product Supply). Experiments were performed in 25 mM Tris-HCl (pH 7.5), 50 mM NaCl, 0.5 mM PMSF, 2 mM TCEP, and 0.04% PEG 20000 at 20 °C. Increasing concentrations of Cy5-labeled duplexes from 0 to 2 μM were added to a fixed Cy3-labeled SRA domain concentration of 0.5 μM. The excitation wavelength was 500 nm. The transfer efficiency was measured from the relative fluorescence intensity of the donor (Cy3) in the absence (F_D) and presence of the acceptor (Cy5) (F_{DA}) with the equation $E = 1 - F_{DA}/F_D$ and plotted as a function of the duplex concentration. The experimental points were fitted by eq 3 adapted from Didier et al.:[53]

$$E = E_f[(1 + K_a([SRA]_{tot} + [ADN]_{tot}) - \{[1 + K_a([SRA]_{tot} + [ADN]_{tot})]^2 - 4K_a^2[SRA]_{tot}[ADN]_{tot}\}^{1/2})/(2K_a[SRA]_{tot})] \quad (3)$$

where $[SRA]_{tot}$ and $[ADN]_{tot}$ are the total concentrations of SRA protein and duplex, respectively, E_F is the final value of FRET efficiency, and K_a is the affinity constant of the protein.

RESULTS AND DISCUSSION

Characterization of 2-Ap-Labeled Duplexes. To site-specifically characterize the complexes of 12 bp DNA duplexes with the SRA domain, the environment-sensitive probe 2-Ap was introduced at various positions (position 3, 5, 5′, 6′, 7, 7′, 8, 8′, or 9) within the duplex ODNs. The central CpG recognition site of the 12 bp duplexes contained either a nonmodified cytosine (NM duplex), a methylated cytosine (HM duplex), or cytosines methylated on both strands (BM duplex) (Figure 1). As compared to native duplexes that exhibited a melting temperature of 55 °C, the melting temperatures of the 2-Ap-labeled duplexes were 10−20 °C lower (data not shown), indicating that although introduction of 2-Ap decreased the stability of the duplexes, their dissociation remained negligible at the experimental temperature (20 °C).

In the absence of the SRA domain, the 2-Ap emission in the labeled duplexes was largely decreased compared to that of free 2-Ap.[38] The quantum yields (QYs) were between 0.006 and 0.025 when the flanking base was a guanine (Figure 1), the most efficient quencher of 2-Ap.[54] Relatively higher QY values were observed only at position 3 (~0.065), probably as a result of the weaker level of stacking of the bases with their neighbors at the end of the duplex.[55,56]

At almost all positions, the QYs of 2Ap were independent of the methylation state of the cytosines. The only exceptions

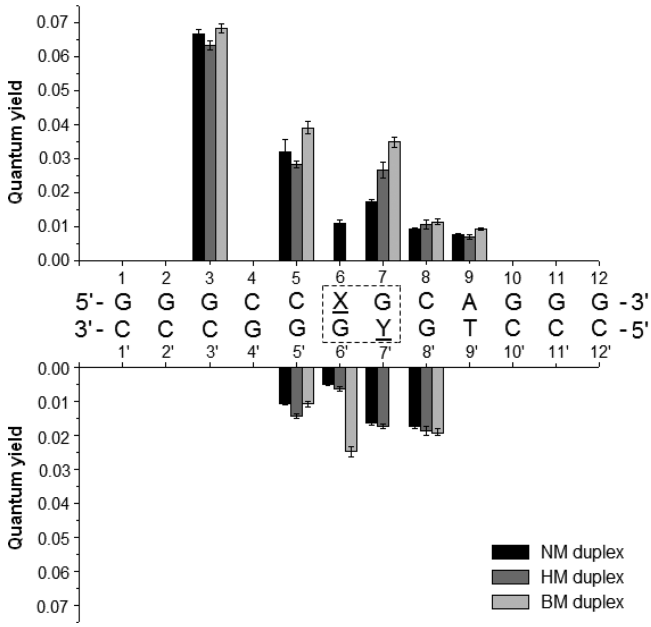

Figure 1. Quantum yields of the 2-Ap-labeled duplexes. The 12 bp ODN contains a single recognition site (dashed square) that is either nonmethylated (NM duplex; X = Y = C), hemimethylated (HM duplex; X = 5mC, and Y = C), or fully methylated (BM duplex; X = Y = 5mC). The 2-Ap residue replaces the natural bases at the indicated positions within the duplexes. Experiments were performed with 3 μM 2-Ap-labeled duplexes in 25 mM Tris-HCl (pH 7.5), 50 mM NaCl, 0.5 mM PMSF, 2 mM TCEP, and 0.04% PEG 20000 at 20 °C. Excitation and emission wavelengths were 315 and 370 nm, respectively.

were at position 7, where the QY was 0.018, 0.027, and 0.039 for NM, HM, and BM, respectively, and at position 6′, where the quantum yield for BM (0.025) was increased by a factor of 4 in comparison to those of HM and NM (0.006). This indicates that the replacement of a cytosine with a methylcytosine at positions 6 and 7′ affects the spectroscopic properties of the 2Ap residues only in their immediate vicinity.

Fluorescence decays of 2-Ap-labeled duplexes (Figure 2A) exhibited four lifetimes, attributed to different conformational states (Figure 2B and Tables S1−S3). This number of lifetimes was found to be the minimal number of lifetimes needed to provide an adequate fit of the fluorescence decays (Figure S1). Moreover, comparison of the QYs and lifetimes of 2-Ap-labeled duplexes and free 2-Ap further revealed the existence of an additional 2-Ap population corresponding to dark species (DS) with lifetimes shorter than the detection limit of our equipment (<0.02 ns).[40,41] The population (α_0) of dark species and the populations ($\alpha_1 + \alpha_2$) associated with the two short lifetimes (τ_1 = 0.04−0.11 ns, and τ_2 = 0.4−0.6 ns) corresponding to the most stacked conformations of the 2-Ap[54] were largely predominant, representing 92−99% for all 2-Ap-labeled duplexes. These large percentages indicate that like the substituted nucleobase, 2Ap is in stacking interactions with its neighbors within the duplex, strongly suggesting that 2-Ap minimally perturbs the duplex structure.

This indicated that the 2-Ap residue efficiently stacked with its neighbors inside the duplex. The only exception was at position 3, where these populations showed a significant decrease to the benefit of populations ($\alpha_3 + \alpha_4$) associated with long lifetimes (τ_3 = 2.8−3.3 ns, and τ_4 = 8.3−10.4 ns). These long lifetimes likely corresponded to unstacked or extrahelical conformations[54] that could accumulate as a result of the lower

DOI: 10.1021/acs.biochem.5b00419
Biochemistry 2015, 54, 6012−6020

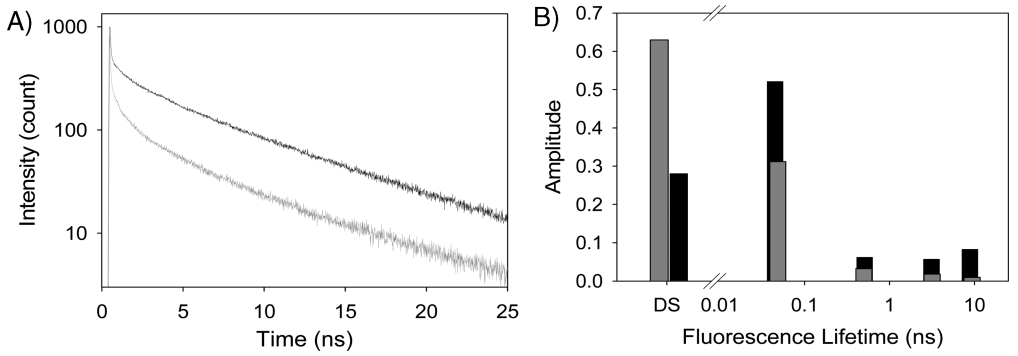

Figure 2. Time-resolved fluorescence decays of 2-Ap-labeled HM duplexes. (A) Fluorescence decays of HM duplexes labeled at position 3 (black) or 8 (gray), taken as representative examples. Experiments were performed with 3 μM 2-Ap-labeled HM duplexes in 25 mM Tris-HCl (pH 7.5), 50 mM NaCl, 0.5 mM PMSF, 2 mM TCEP, and 0.04% PEG 20000 at 20 °C. Excitation and emission wavelengths were 315 and 370 nm, respectively. (B) Time-resolved fluorescence parameters corresponding to the best fit to the fluorescence decays in panel A using the same color code as in panel A. DS corresponds to dark species, with lifetimes that could not be resolved with our setup. The amplitude of the DS and the amplitudes of the various lifetimes were calculated as described in Materials and Methods. Standard deviations are <25% for the lifetimes and the amplitudes.

stability of the duplex at its extremities.[56] Interestingly, the QY increase of the 2-Ap at positions 7 and 6′ with the methylation state of its neighbor cytosines clearly correlated with the increase in the ($\alpha_3 + \alpha_4$) population (Figure 3), suggesting that methylation of cytosines 6 and 7′ can destabilize to some extent its neighboring residues.

The fluorescence anisotropy decays of the 2-Ap-labeled duplex ODNs showed two correlation times φ_1 and φ_2 (Figure 4 and Tables S4−S6). The shorter component, φ_1 (0.19−0.61 ns), was attributed to local rotation of the 2-Ap probe.[54,56] Its high proportion (up to 91%) revealed the high mobility of the 2-Ap base, primarily in its least stacked conformations, corresponding to lifetimes τ_3 and τ_4 that contribute most to the 2-Ap emission.[57] For almost all positions, the slowest correlation time, φ_2, was significantly shorter than the theoretical correlation time (3.2 ns), calculated for the tumbling of a rod-shaped 12-mer DNA duplex (40.7 Å in length and 20 Å in diameter), using eq 2. This indicated a significant contribution of segmental motions and, thus, the high flexibility of the duplexes.[56]

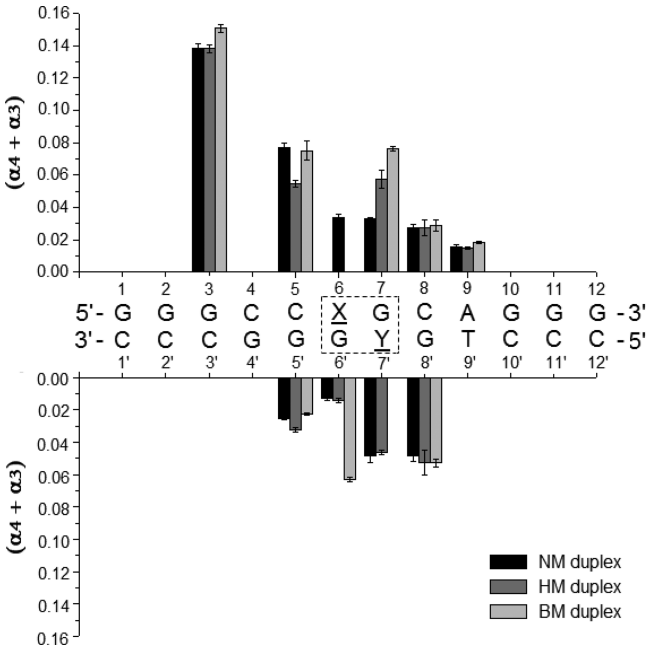

Figure 3. Amplitudes ($\alpha_3 + \alpha_4$) of the two long fluorescence lifetimes of the 2-Ap-labeled duplex ODNs. The 12 bp duplex contains a single CpG recognition site (dashed square) that is either unmethylated (NM duplex; X = Y = C), hemimethylated (HM duplex; X = 5mC, and Y = C), or fully methylated (BM duplex; X = Y = 5mC). The 2-Ap residue substitutes for the natural base at various positions within the ODN sequence. Experiments were performed as described in the legend of Figure 2. The mean values and standard deviations were calculated from the data of at least two experiments.

Effects of the SRA Domain on the Dynamics of the 2-Ap-Labeled Duplexes. Next, we investigated the binding of the SRA domain with the 2-Ap-labeled NM, HM, and BM duplexes. In a first step, FRET experiments using the Cy3-labeled SRA (408−643) domain and Cy5-labeled duplexes were performed to determine the binding parameters under our conditions (Figure 5). In line with previous studies,[5−11] the SRA domain of UHRF1 was found to exhibit a preferential affinity for HM duplexes, with an affinity 4-fold higher than those for NM and BM duplexes (K_d values of 0.08 μM for the HM duplex and 0.28 and 0.25 μM for NM and BM duplexes, respectively). Our observations are in agreement with the previously reported weakened binding of UHRF1 to BM DNA in comparison with that of HM DNA, attributed to the loss of one hydrogen bond in the complex with the BM DNA.[58]

Interestingly, the SRA domain was also observed to bind with a significant affinity (K_d = 0.55 μM) to DNA duplexes lacking the CpG recognition site.[8,58] Competition experiments further revealed that the substitution of a natural nucleobase with a 2-Ap residue only slightly decreased the SRA binding affinity (Figure S2). This conclusion is in line with the facts that replacement of a nucleobase with 2-Ap only minimally affects the DNA structure[26−33,35−37] and that UHRF1 has to recognize CpG sites irrespective of their sequence context. Accordingly, all the subsequent experiments were performed under conditions where at least 80% of the duplexes were bound to SRA.

Interestingly, despite the preferential binding of SRA to HM duplexes, the fluorescence parameters were found to be remarkably similar for all types of duplexes at the various labeled positions (Figures 6 and 7). This suggested that the SRA domain induced similar conformational changes in NM, HM, and BM duplexes and, thus, bound similarly to the three types of duplexes. Except for position 3, far from the CpG recognition site, binding of the SRA domain to 2-Ap-labeled

DOI: 10.1021/acs.biochem.5b00419
Biochemistry 2015, 54, 6012−6020

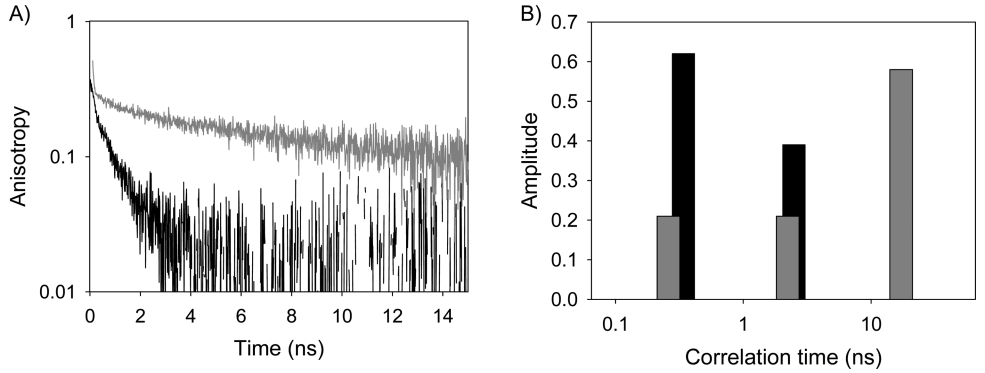

Figure 4. Time-resolved fluorescence anisotropy decays of the HM duplex labeled by 2-Ap at position 8. (A) The anisotropy decay of 3 μM HM duplex labeled with 2-Ap at position 8, taken as a representative example, was recorded in the absence (black) and presence (gray) of 4 μM SRA. Experimental conditions were as described in the legend of Figure 2. (B) Time-resolved fluorescence anisotropy parameters corresponding to the best fit to the decays in panel A, using eq 1 and the same color code as in panel A. Standard deviations are <20% for the correlation times and the amplitudes.

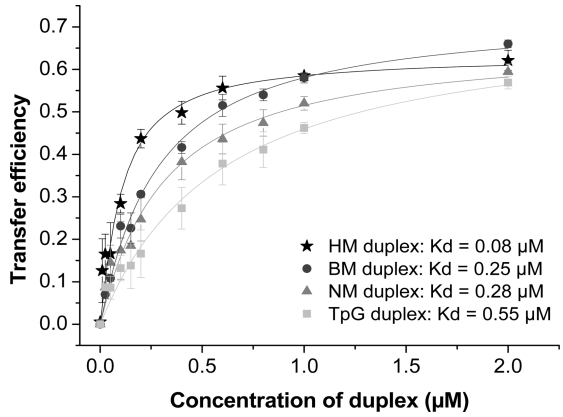

Figure 5. Titration of the SRA domain by DNA duplexes using FRET in solution. Experiments were performed in 25 mM Tris-HCl (pH 7.5), 50 mM NaCl, 0.5 mM PMSF, 2 mM TCEP, and 0.04% PEG 20000 at 20 °C. Increasing concentrations of Cy5-labeled duplexes were added to a fixed Cy3-labeled SRA domain concentration of 0.5 μM. Mean values and standard deviations for at least three experiments are reported on the graph. Except for the TpG duplex (squares) where a thymine substitutes for the methylcytosine in the CpG site of the reference sequence, the duplexes used in this experiment contain a single CpG site that is either nonmethylated (triangles), hemimethylated (stars), or fully methylated (circles). The K_d values of the SRA protein for each of these duplexes are indicated on the graph.

duplexes increased the 2-Ap fluorescence QY by 1.2−5.1-fold, depending on the labeled position (Figure 6A). This change in QY was accompanied by a 2−6 nm blue-shift of its maximal emission wavelength (data not shown), indicating a slight decrease in the polarity of the 2-Ap environment. Time-resolved fluorescence intensity decays revealed that the SRA-induced increase of 2-Ap QY was mainly due to an increase in the populations of the least stacked 2-Ap conformers, which can be seen from the changes in the $(\alpha_3 + \alpha_4)$ values (Figure 6B).

This suggested that through van der Waals and/or hydrogen bonding interactions of its NKR finger (Asp 489, Lys 490, and Arg 491),[5,6,9] the SRA domain slightly destabilized the duplexes, so that the concentrations of less stacked and extrahelical conformations increased. As these conformations, which contribute substantially to the emission spectra of the 2-Ap-labeled duplexes, are in contact with the SRA domain, their environment is less polar than in the free duplexes, readily explaining the aforementioned blue-shift in the emission spectra. Time-resolved anisotropy decays further revealed that SRA strongly restricted the local motion of the 2-Ap bases, as could be seen from the decrease in β_1 values (Figures 4 and 7). The appearance of a third component, φ_3 (~17 ns), fully consistent with the theoretical 16.8 ns value calculated for the tumbling of a 1:1 spherical complex, suggested that the φ_3 component describes only the overall motion of the complex with no contribution of segmental motions, which are now described by the φ_2 component. Thus, the binding of the SRA domain strongly decreased the global flexibility of all duplexes and the local mobility of their bases at the tested positions, likely as a consequence of the multiple contacts formed between the SRA domain and the duplex.[5−7]

The binding of SRA induced the strongest changes in QY, $(\alpha_3 + \alpha_4)$, and β_1 values at positions 7′ and 8 (Figures 6 and 7). Data obtained at position 7′ are consistent with the three-dimensional (3D) structure of the SRA/HM complex showing that the protein NKR finger interacts with the base at position 7′ through a hydrogen bond.[5,6,9] The strong changes in QY at position 8, more pronounced than for position 7′, were more unexpected with respect to the 3D structure, suggesting that SRA could destabilize the 2-Ap at position 8 indirectly through an interaction with the neighbor nucleobases. Interestingly, substitution with 2-Ap of the nonmethylated cytosine at position 6 within the CpG recognition site of the SRA domain was observed to lead to a large decrease in the β_1 amplitude (Figure 7), suggesting a strong interaction of the SRA domain with the nucleobase at position 6 within the SRA/NM complex. Moreover, the SRA-induced spectroscopic changes were highly similar to those at position 8, with $(\alpha_3 + \alpha_4)$ values close to 10% (Table S1). As a flipping out of the 2-Ap residue at position 6 would have been expected to lead to a much stronger accumulation of extrahelical conformations associated with long-lived lifetimes, the small amplitudes of the latter indicate that the SRA domain unlikely flips out the 2-Ap residue at this position. However, as the flipped methylcytosine at position 6 interacts with Tyr 466 and Tyr 478 residues through π-stacking interactions,[5,6,9] a similar flipping of 2-Ap at the same position cannot be excluded. Indeed, as already reported for other proteins, such π-stacking interactions could quench the 2-Ap fluorescence and thus mask the observation of the base flipping.[28,59,60] Noticeably, in spite of the absence of methylated

DOI: 10.1021/acs.biochem.5b00419
Biochemistry 2015, 54, 6012−6020

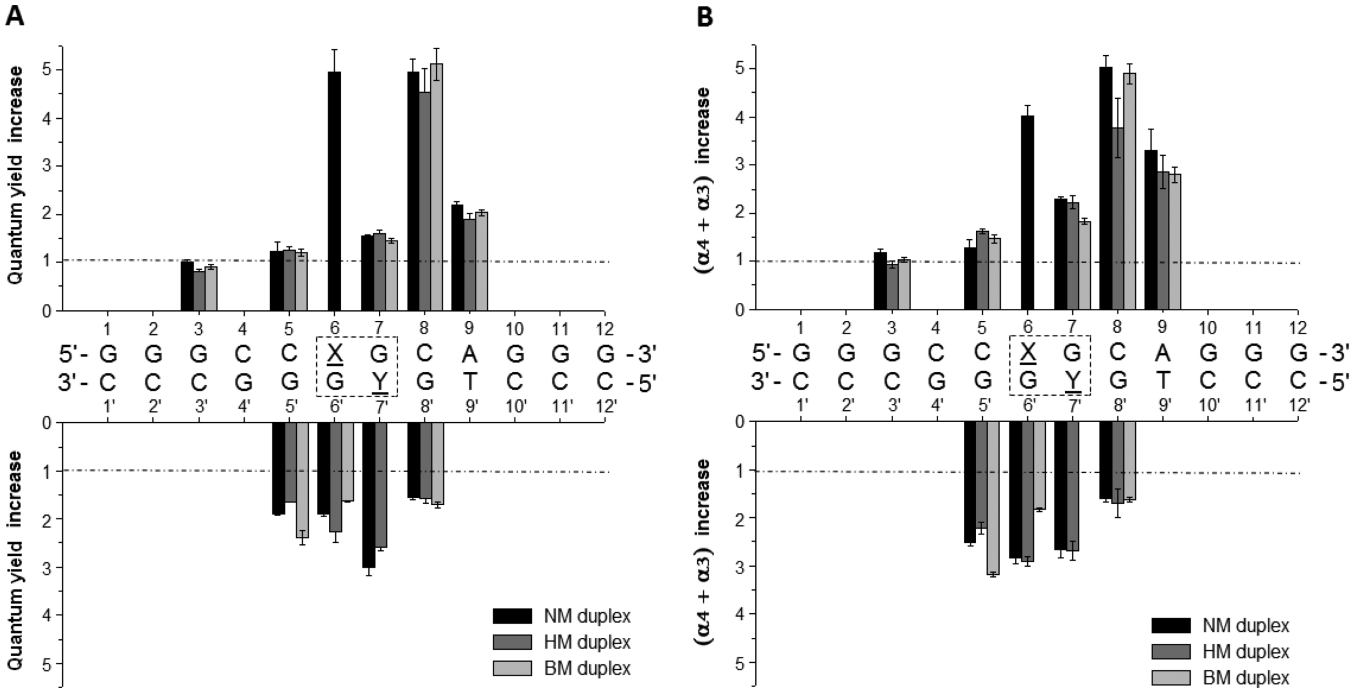

Figure 6. Changes in the quantum yields (A) and the ($\alpha_3 + \alpha_4$) lifetime amplitudes (B) of the 2-Ap-labeled duplex ODNs upon addition of the SRA (408−643) domain. The 12 bp duplex contains a single CpG recognition site (dashed square) that is either unmethylated (NM duplex; X = Y = C), hemimethylated (HM duplex; X = 5mC, and Y = C), or fully methylated (BM duplex; X = Y = 5mC). Experiments were performed with 3 μM 2-Ap-labeled ODNs in the absence or presence of 4 μM SRA domain in 25 mM Tris-HCl (pH 7.5), 50 mM NaCl, 0.5 mM PMSF, 2 mM TCEP, and 0.04% PEG 20000 at 20 °C. Excitation and emission wavelengths were 315 and 370 nm, respectively. For each position in the duplexes, the ratio of the quantum yields (A) or ($\alpha_3 + \alpha_4$) lifetime amplitudes (B) of bound to unbound duplex is represented by a bar, describing the mean value ± the standard deviation of at least two experiments.

cytosine on the NM duplex, the SRA domain shows a much higher perturbation of the base at position 6 as compared to that of the opposite base at position 7′ within the palindromic CpG site (Figure 6). This suggests that the SRA domain is somewhat sensitive to the base context of the recognition site, which favors the binding of the protein on only one side of the duplex.

The binding of SRA to duplexes with 2-Ap replacing the bases at position 5 or 7, directly flanking the target base C6 in the CpG recognition site, induced a similar (~1.4-fold) increase in fluorescence QYs in all three types of duplexes (Figure 6A). However, the β_1 values showed that the local motion of the residue at position 5 and particularly at position 7 was less restricted by the SRA domain in NM duplexes than in HM duplexes (Figure 7). Thus, when the cytosine at position 6 is not methylated, the SRA less stably interacted with its flanking nucleobases, in line with the lower affinity of the SRA domain for the NM duplex as compared to that for the HM duplex. Interestingly, substitution of the G6′ or G7 base with 2-Ap resulted in changes in β_1 amplitudes that were smaller for the BM duplexes than for HM duplexes. Therefore, methylation of the neighboring C7′ residue in BM duplexes seemed to decrease the number of interactions of the nucleobases at positions 6′ and 7 with the NKR finger, probably as a consequence of a steric clash induced by the additional methyl group.[5,6,9,58] In contrast, at position 5′, the SRA domain was found to induce more changes in QY and β_1 values upon binding to the BM duplex as compared to the HM duplex. Thus, in complexes of the SRA domain with BM duplexes, the position of the NKR finger seemed to be shifted, likely as a consequence of the steric hindrance with the methyl group of the C7′ residue. Our data are in agreement with the model proposed by Bianchi et al.[25,58] in which methylation of cytosine 7′ displaces the NKR finger, disrupting the interaction of the SRA domain with the CpG site and slightly strengthening the interactions with other residues.[58] Thus, methyl groups on both cytosines in the BM DNA seem to cause a steric clash that shifts the position of the NKR finger within the DNA, accounting for the decrease in the binding constant of the SRA domain.[5,6,9,58]

Our data further revealed contacts between the SRA domain and the bases at positions 9 and 8′ in all three types of duplexes. However, the limited changes in QY and lifetime data at position 9 were inconsistent with a base flipping at this position as suggested by Hashimoto et al.[9] but rather suggested a limited conformational change in this base. Finally, in contrast to all other tested positions, substitution of the natural base with 2-Ap at position 3 led to no significant changes in the 2-Ap fluorescence parameters upon SRA binding, confirming that this base was located outside of the recognition site of the protein and did not interact with SRA.

■ CONCLUSION

Using the 2-Ap labeling strategy to site-selectively monitor the interaction of duplex ODNs with the SRA domain of UHRF1, we found that the binding of the SRA domain to the nonmethylated, hemimethylated, or fully methylated duplexes induced similar limited changes in the local duplex structure. Indeed, binding of the SRA domain was found to induce a similar limited destabilization in base pairing, as well as a similar restriction of the overall flexibility of the duplexes and the local mobility of the nucleobases, as a likely consequence of the

DOI: 10.1021/acs.biochem.5b00419
Biochemistry 2015, 54, 6012−6020

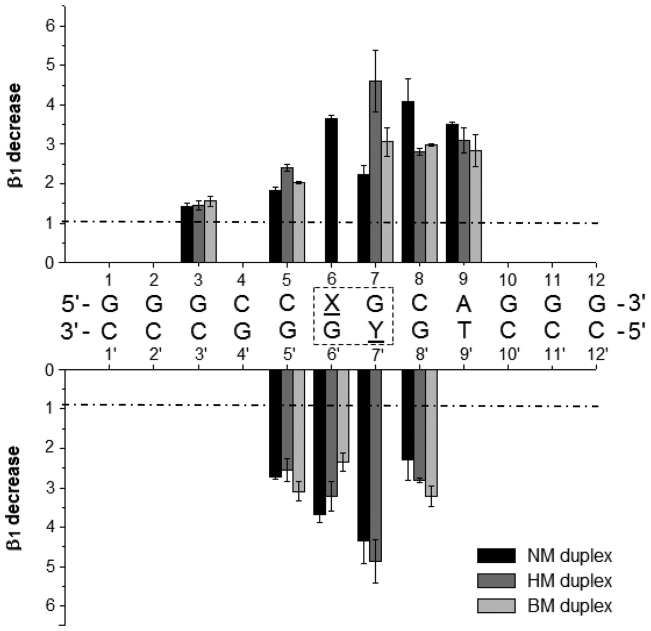

Figure 7. Changes of the β_1 amplitudes associated with the fast rotational correlation times φ_1 of the 2-Ap-labeled duplexes upon addition of the SRA (408−643) domain. Duplexes contain a single CpG recognition site (dashed square) that is either unmethylated (NM duplex; X = Y= C), hemimethylated (HM duplex; X = 5mC, and Y = C), or fully methylated (BM duplex; X = Y = 5mC). Experimental conditions were as described in the legend of Figure 6. For each position in the duplex, the ratio of the β_1 amplitude of unbound to bound duplex is represented by a bar, describing the mean value ± the standard deviation of at least two experiments.

numerous contacts of SRA residues with the duplex observed in the structural data of the SRA/HM complex. Together with the modest preference of the SRA domain for HM, as compared to NM, BM, or even a sequence missing the CpG recognition site (Figure 5), our data are consistent with a "reader" role of the SRA domain that could slide along a DNA duplex to scan for hemimethylated CpG sites.[18,19] This scanning occurs with minimal perturbation in the structure of the contacted nucleotides, as evidenced by the limited changes in the spectroscopic properties of 2-Ap at the different positions within the duplex. These limited changes in the structure of the DNA duplex are fully consistent with NMR data (Protein Data Bank entries 2ZKD, 2ZO0, 3CLZ, 3F8J, 4PW5, 2ZKE, and 2ZKF), showing that the root-mean-square deviation of all SRA binding DNA atoms, including the CpG dinucleotide and 3 bp up- and downstream, is 0.3 Å (data not shown).

The only significant difference observed among NM, HM, and BM duplexes is the greater restriction of the local motion of the residues flanking the methylcytosine in HM as compared to the corresponding residues in NM and BM duplexes. This stronger restriction suggests that these flanking residues are more rigidly bound to SRA, in line with the higher affinity of the SRA domain for HM duplexes as compared to those for the NM and BM duplexes. Moreover, it might be suggested that the tight interaction of the SRA domain in HM duplexes at positions 5 and 7 together with the local conformational changes induced on the complementary strand is instrumental in promoting the binding of DNMT1 in the region of the cytosine to be methylated at position 7′.[25] Noticeably, as a consequence of its low quantum yield and the large amount of dark species in duplexes, 2-Ap may be not the most appropriate tool for revealing fine structural changes among NM, HM, and BM duplexes. Therefore, additional studies with other fluorescent nucleoside analogues are in progress to further investigate this point.

We were not surprised to find a modest difference in the affinity of SRA for BM and HM duplexes. In fact, it is likely that the SRA domain does not need to discriminate between HM and BM as UHRF1 has little chance to meet BM DNA. Indeed, UHRF1 is known to colocalize with PCNA at the replication fork, i.e., at sites of HM DNA generation. Furthermore, it has been suggested that the methylcytosine and the targeted cytosine (by DNMT1) are more likely to swing out successively from the helix, while the DNA is handed over from UHRF1 to DNMT1.[5] This supports the hypothesis that UHRF1 leaves DNA before the catalytic methylation step.

■ ASSOCIATED CONTENT

Supporting Information

The Supporting Information is available free of charge on the ACS Publications website at DOI: 10.1021/acs.biochem.5b00419.

Number of lifetime components required for fitting the time-resolved fluorescence decays of 2-Ap-labeled duplexes (Figure S1), competition between 2-Ap-labeled duplexes and Cy5-labeled duplexes for binding to the SRA domain (Figure S2), steady-state and time-resolved fluorescence parameters of 2-Ap-substituted nonmethylated duplexes (Table S1), steady-state and time-resolved fluorescence parameters of 2-Ap-substituted hemimethylated duplexes (Table S2), steady-state and time-resolved fluorescence parameters of 2-Ap-substituted fully methylated duplexes (Table S3), fluorescence anisotropy decay parameters of 2-Ap-substituted nonmethylated duplexes (Table S4), fluorescence anisotropy decay parameters of 2-Ap-substituted hemimethylated duplexes (Table S5), and fluorescence anisotropy decay parameters of 2-Ap-substituted fully methylated duplexes (Table S6) (PDF)

■ AUTHOR INFORMATION

Corresponding Author

*E-mail: yves.mely@unistra.fr. Telephone: +33-368854263.

Funding

We thank the ANR (ANR-12-BS08-0003-02) and the FRM (DCM20111223038) for financial support. L.K. was supported from the Ministry of Education and Science of Ukraine.

Notes

The authors declare no competing financial interest.

C. Bronner and Y.M. are co-last authors.

■ ABBREVIATIONS

2-Ap, 2-aminopurine; DNMT1, DNA methyltransferase 1; FRET, fluorescence resonance energy transfer; HM, hemimethylated; NM, nonmethylated; BM, bimethylated; ODNs, oligonucleotides; PHD, plant homeo domain; QY, quantum yield; SRA, SET and RING-associated; TTD, tandem Tudor domain; UHRF1, ubiquitin-like containing PHD and RING finger 1.

■ REFERENCES

(1) Jones, P. A., and Liang, G. (2009) Rethinking how DNA methylation patterns are maintained. *Nat. Rev. Genet. 10*, 805−811.

DOI: 10.1021/acs.biochem.5b00419
Biochemistry 2015, 54, 6012−6020

(2) Jurkowska, R. Z., Jurkowski, T. P., and Jeltsch, A. (2011) Structure and function of mammalian DNA methyltransferases. *ChemBioChem 12*, 206−222.
(3) Rottach, A., Leonhardt, H., and Spada, F. (2009) DNA methylation-mediated epigenetic control. *J. Cell. Biochem. 108*, 43−51.
(4) Smallwood, S. A., and Kelsey, G. (2012) De novo DNA methylation: a germ cell perspective. *Trends Genet. 28*, 33−42.
(5) Arita, K., Ariyoshi, M., Tochio, H., Nakamura, Y., and Shirakawa, M. (2008) Recognition of hemi-methylated DNA by the SRA protein UHRF1 by a base-flipping mechanism. *Nature 455*, 818−821.
(6) Avvakumov, G. V., Walker, J. R., Xue, S., Li, Y., Duan, S., Bronner, C., Arrowsmith, C. H., and Dhe-Paganon, S. (2008) Structural basis for recognition of hemi-methylated DNA by the SRA domain of human UHRF1. *Nature 455*, 822−825.
(7) Bostick, M., Kim, J. K., Esteve, P. O., Clark, A., Pradhan, S., and Jacobsen, S. E. (2007) UHRF1 plays a role in maintaining DNA methylation in mammalian cells. *Science 317*, 1760−1764.
(8) Frauer, C., Hoffmann, T., Bultmann, S., Casa, V., Cardoso, M. C., Antes, I., and Leonhardt, H. (2011) Recognition of 5-hydroxymethylcytosine by the Uhrf1 SRA domain. *PLoS One 6*, e21306.
(9) Hashimoto, H., Horton, J. R., Zhang, X., Bostick, M., Jacobsen, S. E., and Cheng, X. (2008) The SRA domain of UHRF1 flips 5-methylcytosine out of the DNA helix. *Nature 455*, 826−829.
(10) Qian, C., Li, S., Jakoncic, J., Zeng, L., Walsh, M. J., and Zhou, M. M. (2008) Structure and hemimethylated CpG binding of the SRA domain from human UHRF1. *J. Biol. Chem. 283*, 34490−34494.
(11) Rottach, A., Frauer, C., Pichler, G., Bonapace, I. M., Spada, F., and Leonhardt, H. (2010) The multi-domain protein Np95 connects DNA methylation and histone modification. *Nucleic Acids Res. 38*, 1796−1804.
(12) Sharif, J., Muto, M., Takebayashi, S., Suetake, I., Iwamatsu, A., Endo, T. A., Shinga, J., Mizutani-Koseki, Y., Toyoda, T., Okamura, K., Tajima, S., Mitsuya, K., Okano, M., and Koseki, H. (2007) The SRA protein Np95 mediates epigenetic inheritance by recruiting Dnmt1 to methylated DNA. *Nature 450*, 908−912.
(13) Unoki, M., Nishidate, T., and Nakamura, Y. (2004) ICBP90, an E2F-1 target, recruits HDAC1 and binds to methyl-CpG through its SRA domain. *Oncogene 23*, 7601−7610.
(14) Arita, K., Isogai, S., Oda, T., Unoki, M., Sugita, K., Sekiyama, N., Kuwata, K., Hamamoto, R., Tochio, H., Sato, M., Ariyoshi, M., and Shirakawa, M. (2012) Recognition of modification status on a histone H3 tail by linked histone reader modules of the epigenetic regulator UHRF1. *Proc. Natl. Acad. Sci. U. S. A. 109*, 12950−12955.
(15) Nady, N., Lemak, A., Walker, J. R., Avvakumov, G. V., Kareta, M. S., Achour, M., Xue, S., Duan, S., Allali-Hassani, A., Zuo, X., Wang, Y. X., Bronner, C., Chedin, F., Arrowsmith, C. H., and Dhe-Paganon, S. (2011) Recognition of multivalent histone states associated with heterochromatin by UHRF1 protein. *J. Biol. Chem. 286*, 24300−24311.
(16) Xie, S., Jakoncic, J., and Qian, C. (2012) UHRF1 double tudor domain and the adjacent PHD finger act together to recognize K9me3-containing histone H3 tail. *J. Mol. Biol. 415*, 318−328.
(17) Rothbart, S. B., Dickson, B. M., Ong, M. S., Krajewski, K., Houliston, S., Kireev, D. B., Arrowsmith, C. H., and Strahl, B. D. (2013) Multivalent histone engagement by the linked tandem Tudor and PHD domains of UHRF1 is required for the epigenetic inheritance of DNA methylation. *Genes Dev. 27*, 1288−1298.
(18) Bronner, C., Fuhrmann, G., Chedin, F. L., Macaluso, M., and Dhe-Paganon, S. (2010) UHRF1 Links the Histone code and DNA Methylation to ensure Faithful Epigenetic Memory Inheritance. *Genet. Epigenet. 2009*, 29−36.
(19) Hashimoto, H., Horton, J. R., Zhang, X., and Cheng, X. (2009) UHRF1, a modular multi-domain protein, regulates replication-coupled crosstalk between DNA methylation and histone modifications. *Epigenetics 4*, 8−14.
(20) Hashimoto, H., Vertino, P. M., and Cheng, X. (2010) Molecular coupling of DNA methylation and histone methylation. *Epigenomics 2*, 657−669.
(21) Hervouet, E., Lalier, L., Debien, E., Cheray, M., Geairon, A., Rogniaux, H., Loussouarn, D., Martin, S. A., Vallette, F. M., and Cartron, P. F. (2010) Disruption of Dnmt1/PCNA/UHRF1 interactions promotes tumorigenesis from human and mice glial cells. *PLoS One 5*, e11333.
(22) Berkyurek, A. C., Suetake, I., Arita, K., Takeshita, K., Nakagawa, A., Shirakawa, M., and Tajima, S. (2014) The DNA methyltransferase Dnmt1 directly interacts with the SET and RING finger-associated (SRA) domain of the multifunctional protein Uhrf1 to facilitate accession of the catalytic center to hemi-methylated DNA. *J. Biol. Chem. 289*, 379−386.
(23) Liu, X., Gao, Q., Li, P., Zhao, Q., Zhang, J., Li, J., Koseki, H., and Wong, J. (2013) UHRF1 targets DNMT1 for DNA methylation through cooperative binding of hemi-methylated DNA and methylated H3K9. *Nat. Commun. 4*, 1563.
(24) Nishiyama, A., Yamaguchi, L., Sharif, J., Johmura, Y., Kawamura, T., Nakanishi, K., Shimamura, S., Arita, K., Kodama, T., Ishikawa, F., Koseki, H., and Nakanishi, M. (2013) Uhrf1-dependent H3K23 ubiquitylation couples maintenance DNA methylation and replication. *Nature 502*, 249−253.
(25) Bianchi, C., and Zangi, R. (2014) Dual base-flipping of cytosines in a CpG dinucleotide sequence. *Biophys. Chem. 187*−*188*, 14−22.
(26) Avilov, S. V., Piemont, E., Shvadchak, V., de Rocquigny, H., and Mely, Y. (2008) Probing dynamics of HIV-1 nucleocapsid protein/target hexanucleotide complexes by 2-aminopurine. *Nucleic Acids Res. 36*, 885−896.
(27) Beck, C., and Jeltsch, A. (2002) Probing the DNA interface of the EcoRV DNA-(adenine-N6)-methyltransferase by site-directed mutagenesis, fluorescence spectroscopy, and UV cross-linking. *Biochemistry 41*, 14103−14110.
(28) Bonnist, E. Y., Liebert, K., Dryden, D. T., Jeltsch, A., and Jones, A. C. (2012) Using the fluorescence decay of 2-aminopurine to investigate conformational change in the recognition sequence of the EcoRV DNA-(adenine-N6)-methyltransferase on enzyme binding. *Biophys. Chem. 160*, 28−34.
(29) Dallmann, A., Dehmel, L., Peters, T., Mugge, C., Griesinger, C., Tuma, J., and Ernsting, N. P. (2010) 2-Aminopurine incorporation perturbs the dynamics and structure of DNA. *Angew. Chem., Int. Ed. 49*, 5989−5992.
(30) Darii, M. V., Cherepanova, N. A., Subach, O. M., Kirsanova, O. V., Rasko, T., Slaska-Kiss, K., Kiss, A., Deville-Bonne, D., Reboud-Ravaux, M., and Gromova, E. S. (2009) Mutational analysis of the CG recognizing DNA methyltransferase SssI: insight into enzyme-DNA interactions. *Biochim. Biophys. Acta, Proteins Proteomics 1794*, 1654−1662.
(31) Eritja, R., Kaplan, B. E., Mhaskar, D., Sowers, L. C., Petruska, J., and Goodman, M. F. (1986) Synthesis and properties of defined DNA oligomers containing base mispairs involving 2-aminopurine. *Nucleic Acids Res. 14*, 5869−5884.
(32) Fazakerley, G. V., Sowers, L. C., Eritja, R., Kaplan, B. E., and Goodman, M. F. (1987) NMR studies on an oligodeoxynucleotide containing 2-aminopurine opposite adenine. *Biochemistry 26*, 5641−5646.
(33) Holz, B., Klimasauskas, S., Serva, S., and Weinhold, E. (1998) 2-Aminopurine as a fluorescent probe for DNA base flipping by methyltransferases. *Nucleic Acids Res. 26*, 1076−1083.
(34) Jones, A. C., and Neely, R. K. (2015) 2-aminopurine as a fluorescent probe of DNA conformation and the DNA-enzyme interface. *Q. Rev. Biophys. 48*, 244−279.
(35) Kenfack, C. A., Piemont, E., Ben Gaied, N., Burger, A., and Mely, Y. (2008) Time-resolved fluorescent properties of 8-vinyl-deoxyadenosine and 2-amino-deoxyribosylpurine exhibit different sensitivity to their opposite base in duplexes. *J. Phys. Chem. B 112*, 9736−9745.
(36) Neely, R. K., Daujotyte, D., Grazulis, S., Magennis, S. W., Dryden, D. T., Klimasauskas, S., and Jones, A. C. (2005) Time-resolved fluorescence of 2-aminopurine as a probe of base flipping in M.HhaI-DNA complexes. *Nucleic Acids Res. 33*, 6953−6960.
(37) Sowers, L. C., Fazakerley, G. V., Eritja, R., Kaplan, B. E., and Goodman, M. F. (1986) Base pairing and mutagenesis: observation of a protonated base pair between 2-aminopurine and cytosine in an

DOI: 10.1021/acs.biochem.5b00419
Biochemistry 2015, 54, 6012−6020

oligonucleotide by proton NMR. *Proc. Natl. Acad. Sci. U. S. A. 83*, 5434−5438.
(38) Ward, D. C., Reich, E., and Stryer, L. (1969) Fluorescence studies of nucleotides and polynucleotides. I. Formycin, 2-aminopurine riboside, 2,6-diaminopurine riboside, and their derivatives. *J. Biol. Chem. 244*, 1228−1237.
(39) Fiebig, T., Wan, C., and Zewail, A. H. (2002) Femtosecond charge transfer dynamics of a modified DNA base: 2-aminopurine in complexes with nucleotides. *ChemPhysChem 3*, 781−788.
(40) Jean, J. M., and Hall, K. B. (2001) 2-Aminopurine fluorescence quenching and lifetimes: role of base stacking. *Proc. Natl. Acad. Sci. U. S. A. 98*, 37−41.
(41) Jean, J. M., and Hall, K. B. (2002) 2-Aminopurine electronic structure and fluorescence properties in DNA. *Biochemistry 41*, 13152−13161.
(42) Jean, J. M., and Hall, K. B. (2004) Stacking-unstacking dynamics of oligodeoxynucleotide trimers. *Biochemistry 43*, 10277−10284.
(43) O'Neill, M. A., and Barton, J. K. (2002) 2-Aminopurine: a probe of structural dynamics and charge transfer in DNA and DNA:RNA hybrids. *J. Am. Chem. Soc. 124*, 13053−13066.
(44) Wan, C., Fiebig, T., Schiemann, O., Barton, J. K., and Zewail, A. H. (2000) Femtosecond direct observation of charge transfer between bases in DNA. *Proc. Natl. Acad. Sci. U. S. A. 97*, 14052−14055.
(45) Delagoutte, B., Lallous, N., Birck, C., Oudet, P., and Samama, J. P. (2008) Expression, purification, crystallization and preliminary crystallographic study of the SRA domain of the human UHRF1 protein. *Acta Crystallogr., Sect. F: Struct. Biol. Cryst. Commun. 64*, 922−925.
(46) Vuilleumier, C., Maechling-Strasser, C., Gerard, D., and Mely, Y. (1997) Evidence and prevention of HIV-1 nucleocapsid protein adsorption onto fluorescence quartz cells. *Anal. Biochem. 244*, 183−185.
(47) Godet, J., Kenfack, C., Przybilla, F., Richert, L., Duportail, G., and Mely, Y. (2013) Site-selective probing of cTAR destabilization highlights the necessary plasticity of the HIV-1 nucleocapsid protein to chaperone the first strand transfer. *Nucleic Acids Res. 41*, 5036−5048.
(48) Godet, J., Ramalanjaona, N., Sharma, K. K., Richert, L., de Rocquigny, H., Darlix, J. L., Duportail, G., and Mely, Y. (2011) Specific implications of the HIV-1 nucleocapsid zinc fingers in the annealing of the primer binding site complementary sequences during the obligatory plus strand transfer. *Nucleic Acids Res. 39*, 6633−6645.
(49) Köllner, M., and Wolfrum, J. (1992) How many photons are necessary for fluorescence-lifetime measurements? *Chem. Phys. Lett. 200*, 199−204.
(50) Ortega, A., and García de la Torre, J. (2003) Hydrodynamic properties of rodlike and disklike particles in dilute solution. *J. Chem. Phys. 119*, 9914−9919.
(51) Brochon, J. C. (1994) Maximum entropy method of data analysis in time-resolved spectroscopy. *Methods Enzymol. 240*, 262−311.
(52) Marquardt, D. (1963) An Algorithm for Least-Squares Estimation of Nonlinear Parameters. *J. Soc. Ind. Appl. Math. 11*, 431−441.
(53) Didier, P., Sharma, K. K., and Mély, Y. (2011) Fluorescence Techniques to Characterise Ligand Binding to Proteins. In *Biophysical Approaches Determining Ligand Binding to Biomolecular Targets: Detection, Measurement and Modelling* (Podjarny, A., Dejaegere, A. P., and Kieffer, B., Eds.) pp 156−199, The Royal Society of Chemistry, London.
(54) Guest, C. R., Hochstrasser, R. A., Sowers, L. C., and Millar, D. P. (1991) Dynamics of mismatched base pairs in DNA. *Biochemistry 30*, 3271−3279.
(55) Avilov, S. V., Godet, J., Piemont, E., and Mely, Y. (2009) Site-specific characterization of HIV-1 nucleocapsid protein binding to oligonucleotides with two binding sites. *Biochemistry 48*, 2422−2430.
(56) Ramreddy, T., Rao, B. J., and Krishnamoorthy, G. (2007) Site-specific dynamics of strands in ss- and dsDNA as revealed by time-domain fluorescence of 2-aminopurine. *J. Phys. Chem. B 111*, 5757−5766.
(57) Sholokh, M., Sharma, R., Shin, D., Das, R., Zaporozhets, O. A., Tor, Y., and Mely, Y. (2015) Conquering 2-Aminopurine's Deficiencies: Highly Emissive Isomorphic Guanosine Surrogate Faithfully Monitors Guanosine Conformation and Dynamics in DNA. *J. Am. Chem. Soc. 137*, 3185−3188.
(58) Bianchi, C., and Zangi, R. (2013) UHRF1 discriminates against binding to fully-methylated CpG-Sites by steric repulsion. *Biophys. Chem. 171*, 38−45.
(59) Lenz, T., Bonnist, E. Y., Pljevaljcic, G., Neely, R. K., Dryden, D. T., Scheidig, A. J., Jones, A. C., and Weinhold, E. (2007) 2-Aminopurine flipped into the active site of the adenine-specific DNA methyltransferase M.TaqI: crystal structures and time-resolved fluorescence. *J. Am. Chem. Soc. 129*, 6240−6248.
(60) Neely, R. K., Tamulaitis, G., Chen, K., Kubala, M., Siksnys, V., and Jones, A. C. (2009) Time-resolved fluorescence studies of nucleotide flipping by restriction enzymes. *Nucleic Acids Res. 37*, 6859−6870.

DOI: 10.1021/acs.biochem.5b00419
Biochemistry 2015, 54, 6012−6020